Ecological Indicators 153 (2023) 110426

Contents lists available at ScienceDirect

Ecological Indicators

journal homepage: www.elsevier.com/locate/ecolind

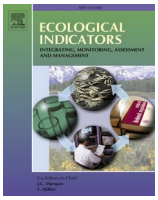

Original Articles

BIOCLIMATIC DROUGHT AND ITS TRENDS IN CALIFORNIA STATE (U.S.)

A. González-Pérez [a,*], R. Álvarez-Esteban [b], Alejandro Velázquez [c], A. Penas [d], S. del Río [d]

[a] Department of Biodiversity and Environmental Management (Botany Area), Faculty of Biological and Environmental Science, University of Leon, Campus de Vegazana s/n. 24071, León, Spain
[b] Department of Economics and Statistics (Statistics and Operations Research Area), Faculty of Economics and Business, University of Leon, Campus de Vegazana s/n. 24071, León, Spain
[c] Centre for Research in Environmental Geography (CIGA) National Autonomous University of Mexico, Old Road to Pátzcuaro 8701, Morelia, Michoacán, Mexico
[d] Department of Biodiversity and Environmental Management (Botany Area), Faculty of Biological and Environmental Science, University of Leon, Mountain Livestock Institute CSIC-UNILEON, Campus de Vegazana s/n. 24071, León, Spain

ARTICLE INFO

Keywords:
Bioclimatology
Climate change
Empirical Bayesian Kriging
Ombroxeric Index
Modified Mann-Kendall
Modified Sen's slope

ABSTRACT

Drought occurs naturally all over the world. Global warming has led an increase in the areas affected by this phenomenon. The study of drought involves the analysis of indicators and indices used to assess changes in the hydrological cycle of a region. A large number of indices developed for drought monitoring are based on meteorological and hydrological variables. This research has applied the Ombroxeric Index for the first time in California. It is based on the concept of ombroxericity: a condition of the territory characterised from an ombrothermic point of view, which can develop in relatively humid areas/zones, depending on the time scale of the study (i.e. monthly, seasonal or annual basis). Temperatures and precipitation from 180 meteorological stations have been considered for a period of observation from 1980 to 2016. In order to know the evolution of this index, a modified trend analysis based on the Mann-Kendall test and a modified Sen slope analysis were used. Empirical Bayesian Kriging was applied as an interpolation technique. Results are presented in both surface and contour maps. California showed a wide range of ombroxeric levels that went from upper strong dry in northern zones, to lower weak arid. Trend results showed an increase in bioclimatic drought throughout the whole State. In addition, summer showed the highest levels on the Ombroxeric Index. An increase in drought trends was observed at the seasonal level, being more pronounced in summer and spring. In both cases are increases in the central (+5 and +3.6 units year^{-1} respectively) and the southern (+4 and +4.5 units year^{-1} respectively) areas of the State. Increasing frequency and severity of droughts could have implications for the management of water resources and the survival of Californian vegetation types, such as conifers.

1. Introduction

Widespread climate change is causing economic and environmental impacts with rapid variability. In fact, global warming is associated with higher temperatures, intensification of hydrological cycles and thus changes in evapotranspiration rhythms (Ajjur and Al-Ghamdi, 2021; Xu et al., 2018). Drought occurs naturally in all parts of the world, as well as in areas of high and low precipitation, and is mostly related to a reduction in the amount of precipitation received over longer period of time such as a month, a season or a year. Moreover, an increase in evapotranspiration could lead to gradual drought events (Mukherjee et al., 2018). In addition, temperatures, strong winds and relatively low humidity play an important role in the occurrence of droughts (Mishra and Singh, 2010). Drought is defined as a shortage of water compared to normal conditions, which can occur in different components of the hydrological cycle (van Loon et al., 2016). It is often subdivided into: meteorological drought (precipitation deficit) (Aghelpour and Varshavian, 2021); agricultural drought (below normal soil moisture levels) (Huang et al., 2017); hydrological drought (below normal surface or groundwater water availability) (Salimi et al., 2021); socioeconomic drought (failure of water resource systems to meet water demand) (Mishra and Singh, 2010); technological drought (reduced yields or water scarcity due to the lack of irrigation technology and/or existing poor water management) (Haque Mondol et al., 2022) and bioclimatic drought or ombroxericity (a condition of the territory characterised from the ombrothermic point of view, which can manifest itself in more

* Corresponding author.
E-mail addresses: agonp@unileon.es (A. González-Pérez), ramon.alvarez@unileon.es (R. Álvarez-Esteban), alex@ciga.unam.mx (A. Velázquez), apenm@unileon.es (A. Penas), sriog@unileon.es (S. del Río).

https://doi.org/10.1016/j.ecolind.2023.110426
Received 13 January 2023; Received in revised form 23 May 2023; Accepted 24 May 2023
Available online 1 June 2023

or less humid territories, depending on the level of study (monthly, seasonal or annual) (del Río et al., 2018).

The study of drought involves the observation of indicators and indices that serve to assess changes in the hydrological cycle of a region. A drought indicator is a measurable variable that can be used to identify the onset, duration and severity of drought (Bachmair et al., 2016; 2015). Drought indicators are formulated to assess hydrological cycles and are applied in a specific region over a period of weeks or months (Yihdego et al., 2019) and consist of categorised single numerical values (Dracup et al., 1980; Marcos-Garcia et al., 2017; Vicente-Serrano et al., 2020). Drought indicators are usually based on direct observations of meteorological, hydrological and agricultural variables, such as rainfall, soil moisture and crop yields (Sepulcre-Canto et al., 2012). On the other hand, a drought index, is a mathematical formula that combines several indicators to provide a quantitative measure of drought conditions (https://www.drought.gov/what-is-drought/monitoring-drought).
Drought indices are calculated from a combination of variables, often using statistical methods to determine how they relate to each other (Yihdego et al., 2019). They also provide quantitative measures that describe the severity, location, timing, and duration of the drought (Heim, 2002). The World Meteorological Organisation (WMO) defines the drought index as "*an index related to some of the cumulative effects of prolonged and abnormal moisture deficiency*" (Heim, 2002). Previous research studies have identified basic criteria that any drought index must meet: (I) the time scale must be appropriate to the question at hand; (II) the index must be a quantitative measure of large-scale, long-term drought conditions; (III) the index must be applicable to the matter; (IV) a highly accurate historical record of the index must be available or computable. In operational drought monitoring, a fifth statement should be added: (V) the index must be computable in near real-time (Friedman, 1957; Heim, 2002; Vu-Thanh et al., 2014).

A large number of drought indices developed for drought monitoring are based on meteorological and hydrological variables (Diodato et al., 2019). The Palmer Drought Severity Index (PDSI) is one example. Originally developed by Palmer (Palmer, 1968) as the Standard Precipitation Index (SPI), it is one of the best known and most widely used drought indices in the US. It is the basis for the operation of the US Drought Monitor (Flint et al., 2018). The US Drought Monitor provides the percentage of the country that is affected by drought. However, the period of record for this index is relatively short and is too brief to assess long-term climate trends (U.S. Environmental Protection Agency, 2022).

Vapour Pressure Deficit (VDP) is another index that has become increasingly useful in drought research projects, although it may be difficult to understand compared to established drought indices such as PDSI (Gamelin et al., 2022). Another index applied to hydrological variables is the Groundwater Drought Index (GGDI) based on NASA's Gravity Recovery and Climate Experiment (GRACE) applied to groundwater in the Central Valley of California, where the authors observed that groundwater drought occurs after drought is expressed in soil moisture (PDSI) and precipitation (SPI) (Thomas et al., 2017).

There is a large body of literature on drought and several drought indices for grasslands and crops have been compared (Otkin et al., 2016). Some of these addressed at satellite monitoring of vegetation dynamics such as the Normalized Difference Vegetation Index (NDVI) which quantifies green vegetation and spatial changes. Some of these indices focus on crops, such as the Evaporative Stress Index (ESI), which is one of the few agricultural drought indicators that reveals actual vegetation stress conditions on the ground. This index does not require information on past precipitation or soil water holding capacity. Instead, the current moisture available to vegetation is derived directly from land surface temperature estimated from satellite data (Anderson et al., 2016; Otkin et al., 2016). A new method for monitoring drought-induced vegetation stress is the Vegetation Drought Response Index (VegDRI) method which represents a new approach to drought monitoring by integrating traditional climate-based drought index information and satellite NDVI measurements of vegetation conditions with different biophysical characteristics (Brown et al., 2013).

The effects of global warming will continue to wreak havoc on water availability on the west coast of the U.S. The southwestern U.S., which includes the states of Arizona, California, Colorado, Nevada, New Mexico and Utah, is experiencing a historic and prolonged drought (Lisonbee et al., 2022). The average annual cost of agricultural losses due to drought in the United States (U.S.) has been estimated to be between $6 and $8 billion (Mirabbasi et al., 2013). There are unprecedented droughts, such as the one that ravaged the U.S. Great Plains in the summer of 2012 (Herrera-Estrada et al., 2017). The severe drought between 2012 and 2016 affected most of the State of California (Griffin and Anchukaitis, 2014; Warter et al., 2021; Williams et al., 2015). Lower inflows (drought periods) mean reduced surface water use, less groundwater storage and no possibility of expanding storage capacity. Particularly in southern California where low supplies are heavily managed, water conveyance capacities showed high values of expansion (Harou et al., 2010). Therefore, drought stress will continue, particularly in California, as evidence by the forest mortality observed in the southern Sierra Nevada (Keen et al., 2022). Plant growth depends on cyclical and seasonal variations in rainfall and temperature, which vary with elevation and distance from the Pacific coast (Barbour et al., 2007). A common feature of drought regions is an increase in hot and dry conditions. However, warmer temperatures are having a greater impact on drought conditions than precipitation in California (Gamelin et al., 2022). There is an urgent need to understand this phenomenon and its direct effects on plant communities. The ability of plants to persist during droughts depends on their access to water resources and also on the physiological mechanisms that regulate water loss (Baguskas et al., 2016).

Knowing how species will respond is essential for effective in biodiversity management and conservation. Furthermore, diverse biological communities and functioning ecosystems are essential for maintaining ecosystem services that support human health (Weiskopf et al., 2020).

However, to our knowledge, no indices have been described that address the direct relationship between natural vegetation and drought as a function of precipitation and temperature over different timescales. Bioclimatology is an ecological science that studies the relationships between climatic conditions and the distribution of living beings and their communities across the globe (Rivas-Martínez et al., 2011).

In this line the Ombroxeric Index (OXI) is a bioclimatic drought index that is used to determine the degree of bioclimatic drought in an area (Álvarez Santacoloma et al., 2022; del Río et al., 2018) and it is based on the Rivas-Martínez Worldwide Bioclimatic Classification System (WBCS) (Rivas-Martínez et al., 2011). It should be noted that its formulation is not mathematically complex, as it can be seen in the Material and Methods section. Furthermore, this index can be applied at different temporal (monthly, seasonal and annual) and spatial scales (local, regional, country, continent…) with appropriate and comparable results. This index sets up the levels of drought in a territory, making it possible to relate them with the presence and distribution of flora and vegetation in the territory. These values of drought, with reciprocity in the vegetation, allow to establish the distribution limits for certain plant communities and to evaluate the effect on them of the possible increase in drought under future climate change.

As a novelty in this research, the Ombroxeric Index is applied for the first time in California, to achieve the following objectives:

- To determine the level of bioclimatic drought by applying the Ombroxeric Index on a broad regional scale at different time scales from 1980 to 2016.

- To analyse the trends of this index in California for the period 1980–2016 on a monthly, seasonal and annual basis.

The assessment and prediction of the bioclimatic drought will provide valuable information for water resource planners and policy makers to deal with the drought outcomes (Mirabbasi et al., 2013). In this way, this research can help environmental managers throughout their local

area (Torregrosa et al., 2013) to take appropriate measures to mitigate the detrimental effects of drought on diverse matters, such as crops and natural plant communities. In this respect, this index is also valid in the agricultural field, as it allows to identify the crop that develops best in a territory with certain values of the Ombroxeric Index. From this work, future research could also be developed to establish the extent of bioclimatic drought in Californian plant communities under the climate change framework.

2. Material and methods

2.1. Study area

This research was carried out in California, which covers an area of 423,955 km^2. It is the third largest state in the United States. California has several major rivers and lakes, including the Sacramento and Colorado Rivers, as well as Lake Tahoe and Searles Lake. The State has two main mountain ranges, the Sierra Nevada and the Coast Range, which give it a varied landscape. The highest Californian peak is Mount Whitney at 4421 m in the Sierra Nevada (Luteyn and Hickman, 1993). It also includes a number of valleys, such as Death Valley and Central Valley. It should be noted that California consists of two southern desert areas, the Mojave and the Sonoran (Colorado), which are part of the Basin and Range geomorphic province.

Furthermore, all this orography (Fig. 1) makes California a place with a very diverse climatology, ranging from desert to subalpine environments (Pathak et al., 2018). There are temperature differences across the State, with inland areas having higher average temperatures than coastal areas. In the basins and valleys adjacent to the coast, the climate is subject to large variations over short distances due to the influence of topography on sea air circulation (Center, 2000). Total annual rainfall varies from 1200 mm in the northern areas to 60 mm in the southern areas. It is characterised by a Mediterranean climate, an important component of which in coastal areas is associated with cooling and humidity in the troposphere (Barbour et al., 2007).

From a bioclimatological point of view, California is divided into three macrobioclimates (Rivas-Martínez et al., 2011). Tropical is found in the Sonora desert. Mediterranean covers more than three-quarters of its surface. By definition, the Mediterranean macrobioclimate has a dry period in the summer (the hottest part of the year). Precipitation (mm) is less than or equal to twice the temperature (expressed in centigrade) ($P \leq 2T$) for at least two consecutive summer months. The Temperate macrobioclimate is found in the Klamath highland.

Barbour et al. (2007) provide valuable insights into the variety of

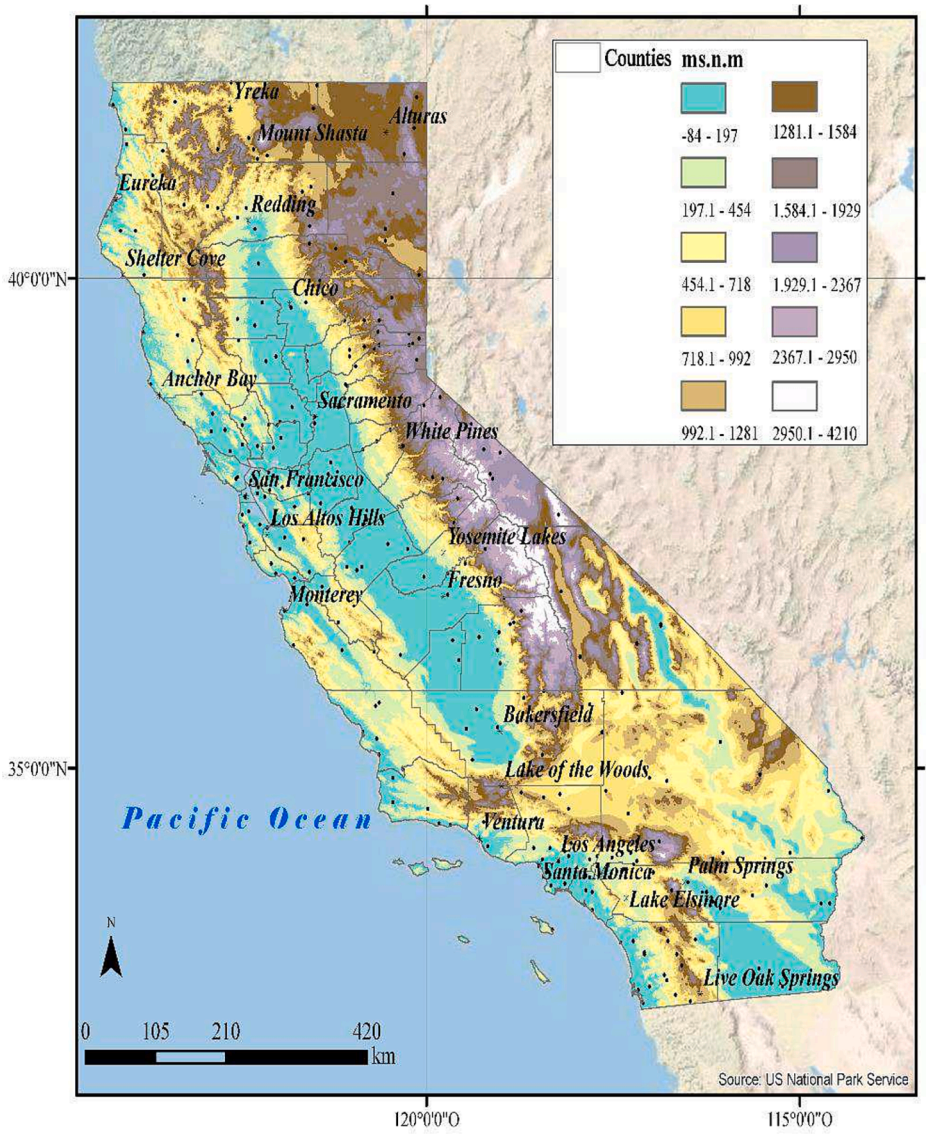

Fig. 1. Physical map of California with the meteorological stations used in this research (●).

vegetation types that can be found in California. Some of them are chaparral, desert, grasslands and redwood forest which are explained in more detail bellow:

Chaparral, a common type of scrub, thrives in various regions of California, particularly in the coastal ranges and inland valleys. It is characterised by the presence of distinctive species such as Ceanothus cuneatus (Hook.) Nutt., *Arctostaphylos canescens* Eastw., and *Quercus agrifolia* Nee. The deserts of California, on the other hand, are home to a specialised vegetation adapted to the harsh conditions. Amongst the most prevalent species found in these arid landscapes are *Coleogyne ramosissima* Torr., *Yucca brevifolia* Engelm., and *Larrea tridentata* (DC.) Coville.

Grasslands can be found in different parts of the state, including the Central Valley and the coastal plains. Notable species within California's grasslands include *Festuca californica* Vasey and *Nassella pulchra* (Hitchc.) Barkworth. Moreover, across locations such as the Central Valley and the coastal plains, Wetlands, vital ecosystems, are scattered. Some of the species commonly found in these wetlands are *Typha latifolia* L., Spergularia marina (L.) Besser, and *Cuscuta salina* Engelm.

The redwood forest, a magnificent coniferous forest, flourishes along the coast, especially in the northern part of the state. The towering *Sequoia sempervirens* Endl. is the iconic tree that dominates this forest Other forests, such as coniferous and mixed forests, are notable for their abundant presence of Douglas fir (*Pseudotsuga menziesii* (Mirb.) Franco), Tanoak (*Lithocarpus densiflorus* (Hook. & Arn.) Rehder), cypress Lawson's (*Chamaecyparis lawsoniana* (A. Murray bis) Parl.), and the oak (*Quercus chrysolepis* Liebm). These forests thrive in the mountain ranges, particularly in the high northern areas and in the Sierra Nevada.

The remarkable variety of topography, vegetation, and climate throughout the state contributes to the rich diversity of California's soil, forming a complex and interconnected web of life and natural wonders.

2.2. Data

For each meteorological station, Climate data values for precipitation and average temperature from 1980 to 2016, were obtained from the WRCC ("Western Regional Climate Center," 2020) website. Initially, 350 meteorological stations were selected. These were chosen based on criteria of completeness, length and homogeneity across most of the State (He and Gautam, 2016). Only stations with less than 10 % of missing values were chosen. The gaps were filled with the corresponding monthly long-term mean value (Ríos Cornejo et al., 2015). Afterward, analysis of the homogeneity of the data was verified (Blöschl et al., 2019; Gocic and Trajkovic, 2013; Karmeshu, 2015; Song et al., 2019). In this study it was determined by the Run test (Thom, 1966) at a 95% confidence level. It was not necessary for the analysed series to follow normal criteria, which has been used previously in other climate studies (González-Pérez et al. (2022a; b); Meseguer-Ruiz and Sarricolea, 2017; Río et al., 2013). Finally, climate variables such as precipitation and mean temperature of 180 stations were chosen for the study (Fig. 1). Besides, we added their elevation values and geographical in order to be able to present the results on maps. In addition, the Ombroxeric Index was calculated for each of the meteorological stations (del Río et al., 2018).

2.3. Ombroxeric index

The Ombroxeric Index is based on the concept of ombroxericity: a condition of the territory characterised from an ombrothermic point of view, that can develop in fairly humid areas, depending on the time scale of the study (monthly, seasonal or annual) (del Río et al., 2018; Ferreiro-Lera et al., 2022). This also considers other index, the annual Ombrothermic Index [Io = (Pp/Tp)*10], which relates the amount of annual Positive precipitation (Pp) and annual Positive temperature (Tp) throughout the territory. Both positive temperature and positive precipitation are directly linked to vegetation, and are measured by taking positive values of temperature and corresponding precipitation, i.e. the conditions in which plant growth is possible (Rivas-Martínez et al., 2011).

This index was analysed at monthly, seasonal and annual levels. California has four seasons which are spring (March, April and May), summer (June, July and August), autumn (September, October and November) and winter (December, January and February). Henceforward those periods will be named in the text as MAM, JJA, SON and DJF.

The equation for calculating the Ombroxeric Index on a monthly scale is as follows:

$$OXIi = 360 - (100^{*}Ioi) \quad (1)$$

where OXI_i is the monthly Ombroxeric Index

and Io_i is the Ombrothermic Index of month i (i = 1, 2, … 12), where i = 1 January and i = 12 December.

Equations on seasonal and annual time-scales are as follows:

$$Winter\ Ombroxeric\ Index(OXI_w): \quad OXI_w = OXI_{12} + OXI_1 + OXI_2; \quad (2)$$

$$Spring\ Ombroxeric\ Index(OXI_{spr}): \quad OXI_{spr} = OXI_3 + OXI_4 + OXI_5; \quad (3)$$

$$Summer\ Ombroxeric\ Index(OXI_{sum}): \quad OXI_{sum} = OXI_6 + OXI_7 + OXI_8; \quad (4)$$

$$Autumn\ Ombroxeric\ Index(OXI_{aut}): \quad OXI_{aut} = OXI_9 + OXI_{10} + OXI_{11}. \quad (5)$$

$$Annual\ Ombroxeric\ Index(OXI_a): \quad OXIa = \sum_{i=1}^{12} OXIi \quad (6)$$

where i = 1 January and i = 12 December

Table 1 shows the different types and levels that characterise the index. The numerical values of the levels are also shown, noting that those values are summative for the seasonal and annual total.

Table 1
Ombroxeric index levels and values taken from del Río et al. (2018) & Ferreiro-Lera et al. (2022).

Ombroxeric Index values			
Ombroxerotypic levels	Monthly (OXI_i)	Seasonal (OXI_{spr}, OXI_{sum}, OXI_{aut}, OXI_w)	Annual (OXI_a)
Upper weak dry	1–40	1–120	1–480
Upper strong dry	40–80	120–240	480–960
Lower weak dry	80–120	240–360	960–1440
Lower strong dry	120–160	360–480	1440–1920
Upper weak semiarid	160–180	480–540	1920–2160
Upper strong semiarid	180–210	540–630	2160–2520
Lower weak semiarid	210–240	630–720	2520–2880
Lower strong semiarid	240–260	720–780	2880–3120
Upper weak arid	260–280	780–840	3120–3360
Upper strong arid	280–290	840–870	3360–3480
Lower weak arid	290–310	870–930	3480–3720
Lower strong arid	310–320	930–960	3720–3840
Upper hyperarid	320–330	960–990	3840–3960
Lower hyperarid	330–340	990–1020	3960–4080
Upper ultrahyperarid	340–350	1020–1050	4080–4200
Lower ultrahyperarid	350–360	1050–1080	4200–4320

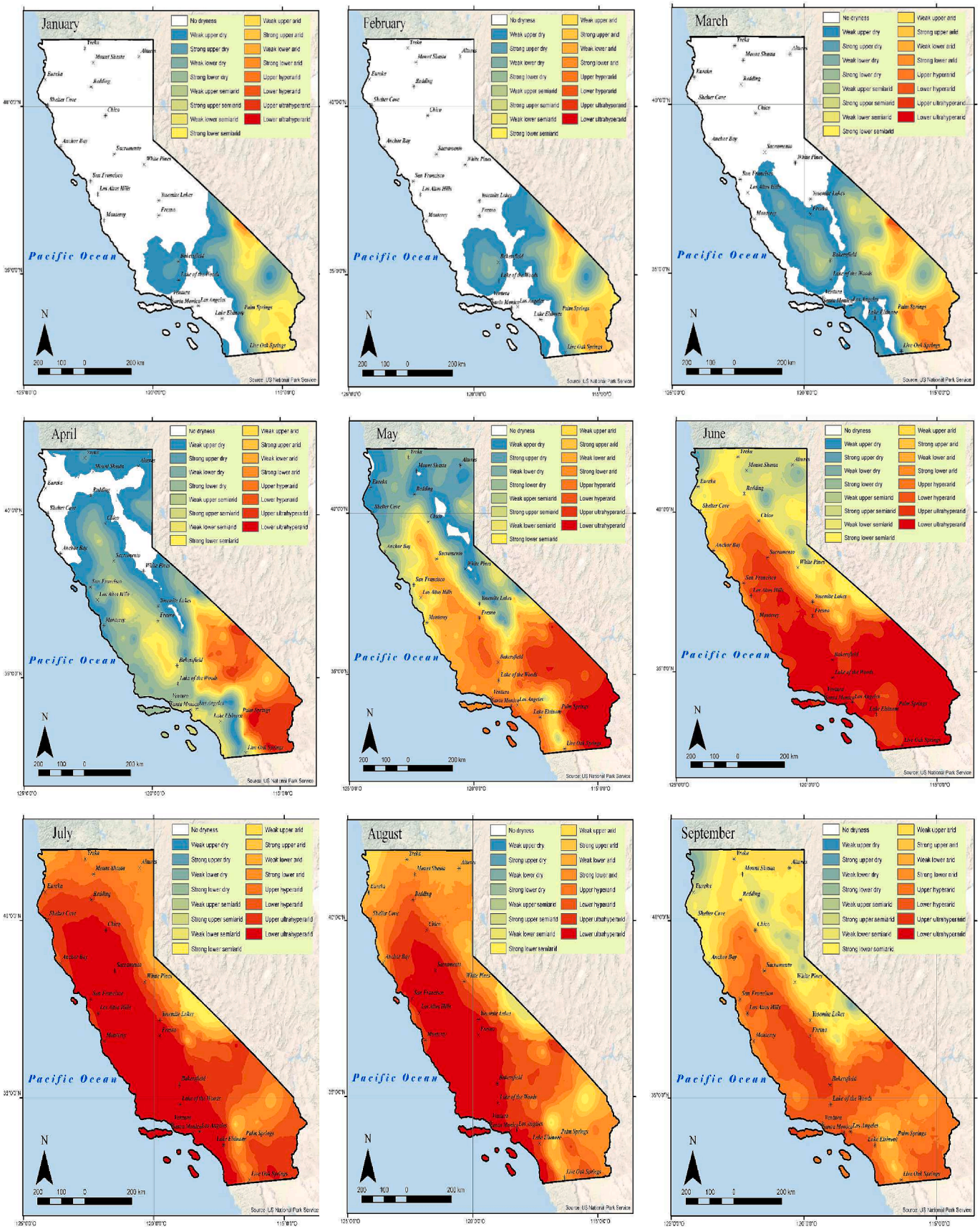

Fig. 2. Ombroxericity levels over the State of California on a monthly, seasonal and annual time scale.

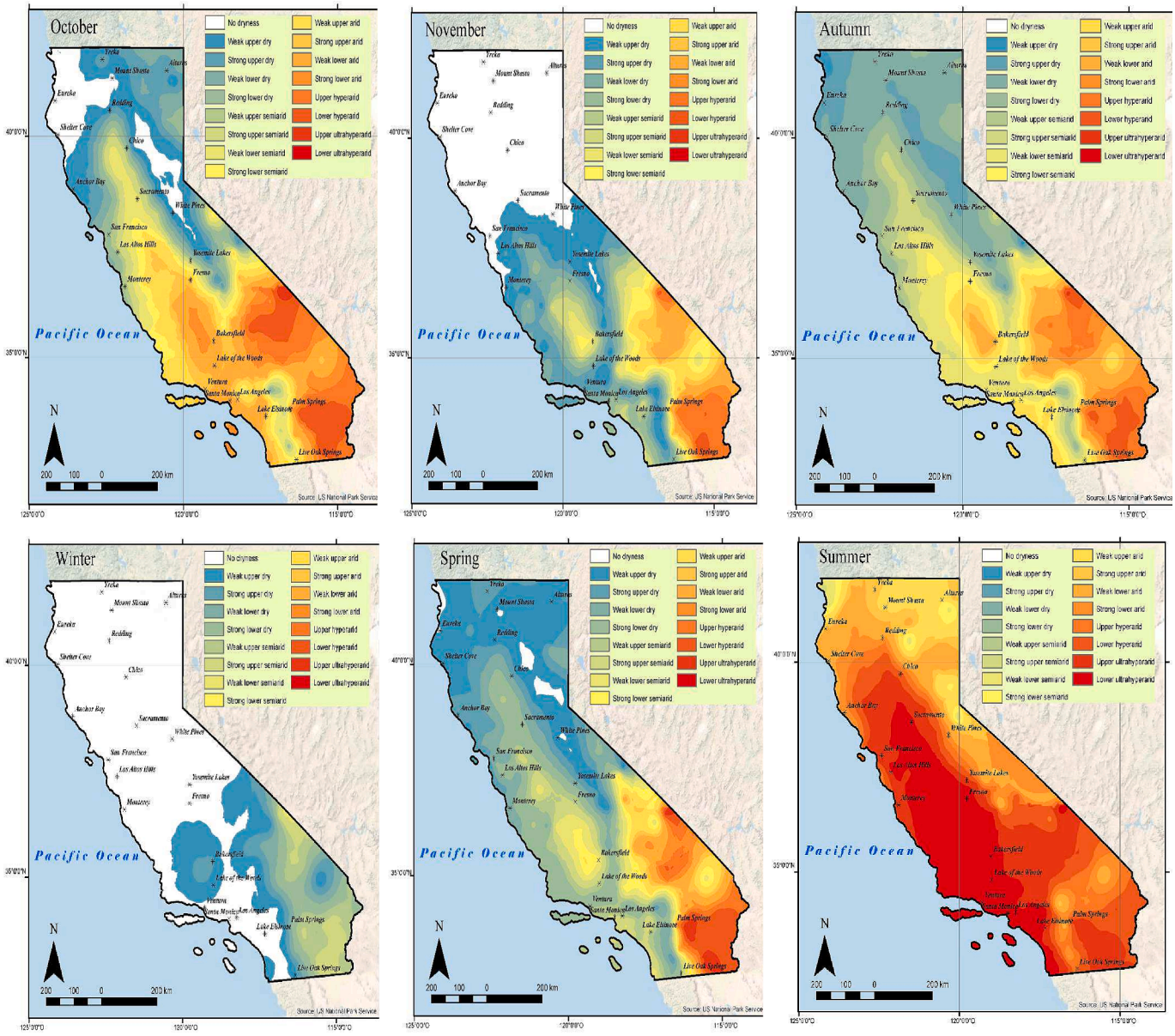

Fig. 2. (*continued*).

2.4. Trend analysis

To achieve one of the objectives of this work, we calculated the trend of the Ombroxeric Index. We used both the modified Sen's slope method and the modified Mann-Kendall test (Liu et al., 2020; Patakamuri and O'Brien, 2021; von Storch, 1995) to obtain the slope results from the 180 stations using the R package version 4.1.0. The Sen slope estimator is a non-parametric procedure that estimates the variation per unit of time in a series where there is a linear trend.

Trend analysis was carried out at monthly, seasonal and annual levels. The non-parametric modified Mann-Kendall test was applied to estimate trends and their statistical significance. The Kendall tau test is one of the most commonly used non-parametric tests to detect trends in environmental time series data, (González-Pérez et al., 2022b; He and Gautam, 2016; Kukal and Irmak, 2016; Meseguer-Ruiz and Sarricolea, 2017; Peña-Angulo et al., 2021).

Statistical interpolation of the values is necessary for some specific regions because long-term average weather observations come from scattered, discrete and unevenly distributed weather stations. These discrete data need to be spatially extended to reflect the continuous and gradual change in the climate pattern (Ghazal, 2019). Empirical Bayesian Kriging (EBK) outperforms classical geostatistical methods and attempts to account for the uncertainty introduced in the semivariogram in ordinary kriging (Gupta et al., 2017). In order to achieve this, the semivariogram parameters in EBK are estimated using the restricted maximum likelihood. In this research, 100 simulations have been selected, meaning that the program runs 100 times and creates one semivariogram each time. This information is used to quantify the probability of a particular simulation occurring (Gribov and Krivoruchko, 2020; Gupta et al., 2017; Krivoruchko, 2012; Krivoruchko and Gribov, 2019; Li et al., 2020). To guide this interpolation, ArcGIS 10.8© (Environmental Systems Research Institute (ESRI), 2019) software was used, and in particular, the EBK geoprocessing tool was applied. In addition, the same software was used to create trend contour maps of the Ombroxeric Index, and areas of statistical significance (95% confidence level) were overlaid on the contour maps.

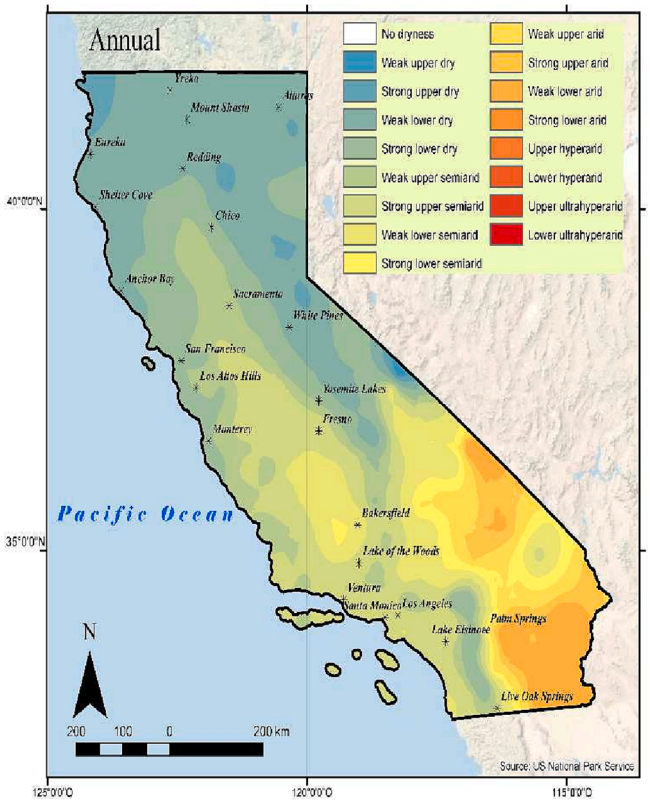

Fig. 2. (*continued*).

3. Results and discussion

3.1. Ombroxeric index levels

In this section, Fig. 2 shows the results of the monthly, seasonal and annual Ombroxeric Index (OXI) and allows us to observe the different levels of the bioclimatic drought that exist in the different areas of the State of California. In general, an increase in the value of the Ombroxeric Index is observed in the southern territories in the State. The highest levels of drought are reached during the summer months in a large part of the territory under study.

3.1.1. Monthly analysis

First of all, it should be noted that no bioclimatic drought was found in December, in fact nearly all meteorological stations showed a zero value for the OXI_i and for this reason there is no map for this month in Fig. 2. Nevertheless, bioclimatic drought can be found in the southern parts of the State in January. OXI_i values range go from weak lower arid (294 units) in Death Valley, to weak upper dry (7 units) in San Diego, Chula Vista and around Inyokern. In the rest of the State there is no bioclimatic drought during this month (Fig. 2). In the San Joaquín Valley, Bakersfield and its surroundings, especially in Maricopa, we found increases in the value of OXI_i in February, reaching the level of strong lower dry (124 units). During the same month, drought values increased to weak lower arid (295 units) in the territories surrounding Death Valley. In the southernmost part of the State, the Sonoran Desert, drought values also increased to weak lower arid in El Centro (300 units) (González-Pérez et al. (2022a; b); Kam and Sheffield, 2016).

Turning to our March results, it is worth noting that the drought extends through the San Joaquin Valley and south of the Sacramento Valley reaching upper dry levels in Turlock (13 units) and San Luis (61 units). Much of the southern half of the State is affected by drought, even more so in the south. The highest values of OXIi, as in previous months, are found in Imperial, El Centro and Death Valley, which have shown an upper hyperarid level (325–328 units). This is not the case, for example, in the San Gabriel, San Bernardino and Santa Rosa mountain ranges. There is a pronounced bioclimatic drought in California in April except for on the highest peaks of Sierra Nevada, Shasta Mountain and the Pacific Northwest coast. Notably, there is a marked change from the previous month. A large increase in OXI_i values is observed in the San Joaquin and Sacramento Valleys. In these areas, there are drought levels ranging from strong lower dry in Sacramento (126 units) and Orland (128 units), going through strong upper semiarid level in Madera (181 units) and Modesto (188 units), to weak upper arid in Corcoran (260 units). The general pattern of drought intensifies in the southern part of the State (Fig. 2). Bioclimatic drought ranges from strong upper arid level in Los Angeles (185 units), upper hyperarid in Barstow (327 units) to upper ultrahyperarid in Death Valley (346 units) and Brawley (350 units). In May, the only areas without bioclimatic drought are the summit of Mount Shasta, the higher elevations of the northern Sierra Nevada, and the surrounding areas of Crescent City. Virtually all of the southern territories of the State exceed the strong upper arid level, with the exception of the southern San Bernardino Mountains. In these areas we found weak lower semiarid levels in Idyllwild (225 units) to weak upper arid at Henshaw (262 units) (González-Pérez et al. (2022a; b)).

If we now turn to the OXI_i results for the month of June, we find that the entire State shows drought to a greater or lesser extent. Highlighted in bright red on the map (Fig. 2) are the large number of territories in the southern California with a drought level of lower ultrahyperarid (359 units). The lowest drought values are observed in the north of the State and on the northwest coast (42 units). July is the month with the most severe drought in the State of California. It is striking how the ultra-hyperarid levels on the coast become less severe as one moves inland. The lowest drought level for this month is the strong lower semiarid (249 units) at Twin Lakes. in August, however, ultrahyperarid levels are located mainly in the San Joaquin and Sacramento Valleys. Most of these areas showed lower ultrahyperarid level, such as in San Francisco (356 units), Los Banos (357 units) and Fresno (358 units). The lowest value of

OXI_i (weak lower semiarid) is found in Big Bear Lake (217 units).

In September, the northern of the State showed a marked decrease in OXI_i values and therefore in drought intensity. In fact, the lowest level, strong upper dry, is reached (68 units) in the vicinities of Klamath. The highest values are only found in two places, Bakersfield (350 units) and Concord (351 units), which have the lower ultrahyperarid level. Southern California much of the area is in the weak lower arid level with values ranging from 290 to 310 units. In the northern part of the state, the drought receded during October in areas around Klamath, Crescent City, Eureka, Nevada City and Paradise, amongst others. In those territories no drought is found (0 units). In mid-southern California semiarid levels are found from Oakland (169 units), Berkeley (172 units), Palomar Mountain (193 units) to San Jose (257 units). The highest values of bioclimatic drought (lower ultrahyperarid) are found in the southeast of the State particularly in Palm Springs (331 units) and Death Valley (351 units). Drought disappeared in the north of the State during November. Nevertheless, southern locations showed elevated values of OXI_i reaching the hyperarid level in Imperial (331 units) and El Centro (332 units).

3.1.2. Seasonal analysis

Spring results show that upper ultrahyperarid levels are reached in places such as Death Valley (1031 units), Imperial (1032 units) and El Centro (1039 units). On the southwest coast of California along the San Joaquin and Sacramento Valleys, drought scores are less pronounced, ranging from weak lower dry at Clearlake (258 units), through Weak upper semiarid at Laguna Beach (520 units) to weak upper arid levels at Buttonwillow (789 units) these results are somehow related to the Drought Monitor Index which shows similar areas of extreme and severe drought (https://droughtmonitor.unl.edu/). No drought is found in this season in Sierra Nevada locations such as Downieville, Strawberry Valley and Bowman, as well as Mount Shasta, Klamath and Crescent City (Fig. 2). These results are consistent with previous research that claimed there was a clear warming throughout the State and an increase in precipitation in northern areas (González-Pérez et al. (2022a; b)).

In summer (Fig. 2), the lower ultrahyperarid zone is reached in places such as in San Diego (1062 units) and Paso Robles (1065 units). These values of the Ombroxeric Index in summer make it the season with the greatest bioclimatic drought, in accordance with the climatology of areas with a Mediterranean climate (Corbin et al., 2005; Dong et al., 2019b; Seager et al., 2019). The lowest value of the Ombroxeric Index is observed at Twins Lakes (547 units), with a level of strong lower semiarid. Intermediate values are found in the northwestern parts such as Boca (804 units) and Tulelake (831 units) with a level of weak upper arid. This is particularly important given that summer streamflow is projected to continue to decline in basins and rivers such as those ones in The Sierra Nevada (Chang and Bonnette, 2016). Although the focus is on a different time period, comparable results were found showing that temperature plays an important role in the development of drought with increasingly variable precipitation (Shukla et al., 2015). It is worth noting that warmer temperatures lead to a decrease in the snowpack (Hamlet et al., 2005), which is a crucial water source for California during the summer months. Snow acts as a natural reservoir, providing a steady stream of water during the warmer months, which can help alleviate drought conditions. However, as temperatures have risen, snowpack levels have decreased, leading to more severe drought events (Shukla et al., 2015).

Looking at the autumn results, California shows drought in some places (Fig. 2). The lowest values are found in the northern part of the State, located in the areas around Eureka and Crescent City with a weak upper dry level. In contrast, the highest OXI_i values are found in the southern areas of California. The locations adjacent to Death Valley and Downtown reach the upper ultrahyperarid level (1035 units). Isolated areas (weak lower dry) of this level are observed at higher altitudes in the Laguna and San Bernardino mountains.

Due to the absence of bioclimatic drought in December, the results of the winter analysis are similar to those of January and February, which is supported by a previous research claiming that the winter drought risk in California has changed to a higher risk, especially in Southern California (Kam and Sheffield, 2016). During this season, the highest values of OXI_i are found in Death Valley and Greenland Ranch (589 units), which reach the strong upper semiarid level. This is directly related to recent research results where there is a positive temperature trend and a negative precipitation trend in southern areas during this season (González-Pérez et al. (2022a; b)).

3.1.3. Annual analysis

With regard to the annual results of bioclimatic drought, we observe severe bioclimatic drought in the southern areas. The highest values are located in Death Valley and el Centro with lower weak arid level (3700 units). The central valley showed high values of bioclimatic drought up to the weak upper semiarid level, which is consistent with other research that have shown that high evapotranspiration rates are due to several factors such as high temperatures and extensive agriculture (Diffenbaugh et al., 2015; Famiglietti et al., 2011). The northern territories of Crescent City and the Klamath Mountains show bioclimatic drought at an upper strong dry level (680 units). These results are closely related to previous research that found a significant increase in temperature (Cordero et al., 2011; González-Pérez et al., 2022a; Goss et al., 2020). Moreover, California has experienced a decrease in precipitation levels, leading to drought conditions (Dong and Leung, 2021; González-Pérez et al., 2022b; Trenberth, 2008).

3.2. Trends of the ombroxeric index

As has been explained above, the Ombroxeric Index allows us to detect bioclimatic drought. Thus, with trend results, we can understand what has happened in the State of California during the study period. Focusing on our results presented in Figs. 3-6, negative trends are found in up to 25% of the meteorological stations in April, May and Spring. A large number of the stations (50% to 85%) showed no trend, depending on the month. In the case of December, as shown above, no bioclimatic drought is found but a few meteorological stations showed trend. In relation to the annual trend value, we observe a large percentage of stations (82%) showing positive trends for the Ombroxeric Index. In addition, 80% of the stations showed positive trends in autumn.

3.2.1. Monthly trends

Starting with the winter months in which this phenomenon currently occurs (excluding December), we can see that the trend increases in both January and February in Southern California (Fig. 7). In January, the largest increase in the index (+4.4 units $year^{-1}$) is observed in the San Bernardino Mountains. In addition, there is a positive trend (+2.8 units $year^{-1}$) in the areas of the Mojave and Sonoran deserts. However, in February, the trend value of the index is lower than in the previous month and the areas where this trend is observed are more localised in the south of the State, in the Imperial Valley (2.4 units $year^{-1}$) and in the Mojave Desert.

An increase in the trend of the Ombroxeric Index was observed in March (Fig. 4), particularly in the central part of California (Fig. 7). Examples of this are the trend values reached in the San Joaquin Valley (4.2 units $year^{-1}$), Fresno (1.54 units $year^{-1}$) and Los Banos (1.5 units $year^{-1}$). In particular, there was an increase in the southern areas where trends reached values of +3.6 units $year^{-1}$. This is the case for the southern Coast Ranges, the San Bernardino Mountains (+4.2 units $year^{-1}$), and the southern part of the Sierra Nevada (+3 units $year^{-1}$), in the White Mountains and Mount Whitney (+3 units $year^{-1}$). These results are consistent with the findings of positive temperature trends and markedly decreasing trends in precipitation for this month over a comparable period (González-Pérez et al. (2022a; b)).

It is striking what happens when we focus on the analysis of trends during April in the State. The trend results showed a decrease in drought

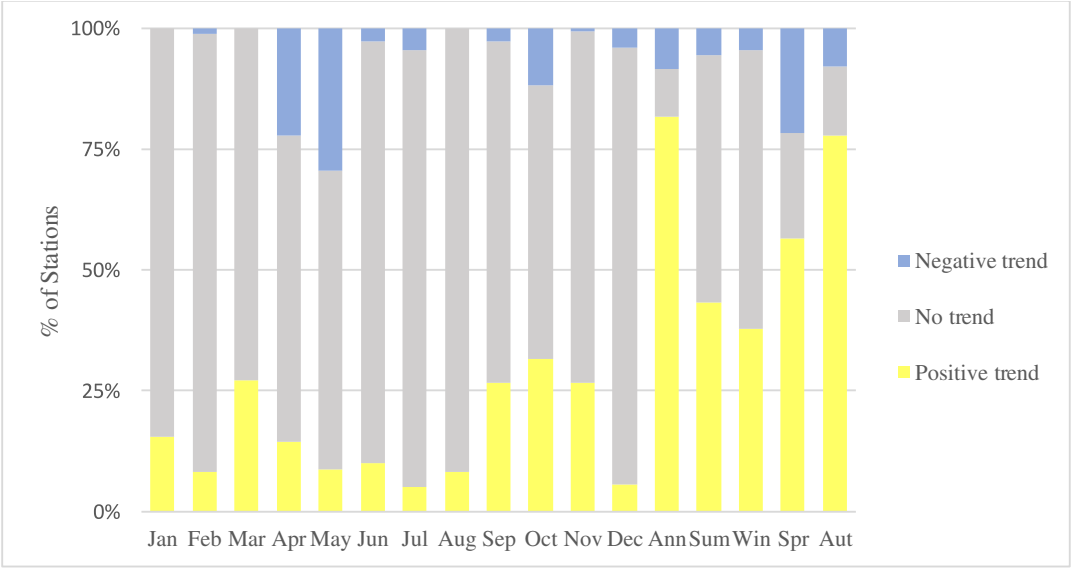

Fig. 3. Percentage of meteorological stations with positive and negative trends (monthly, seasonal and annual scale) in the State of California during the period 1980–2016.

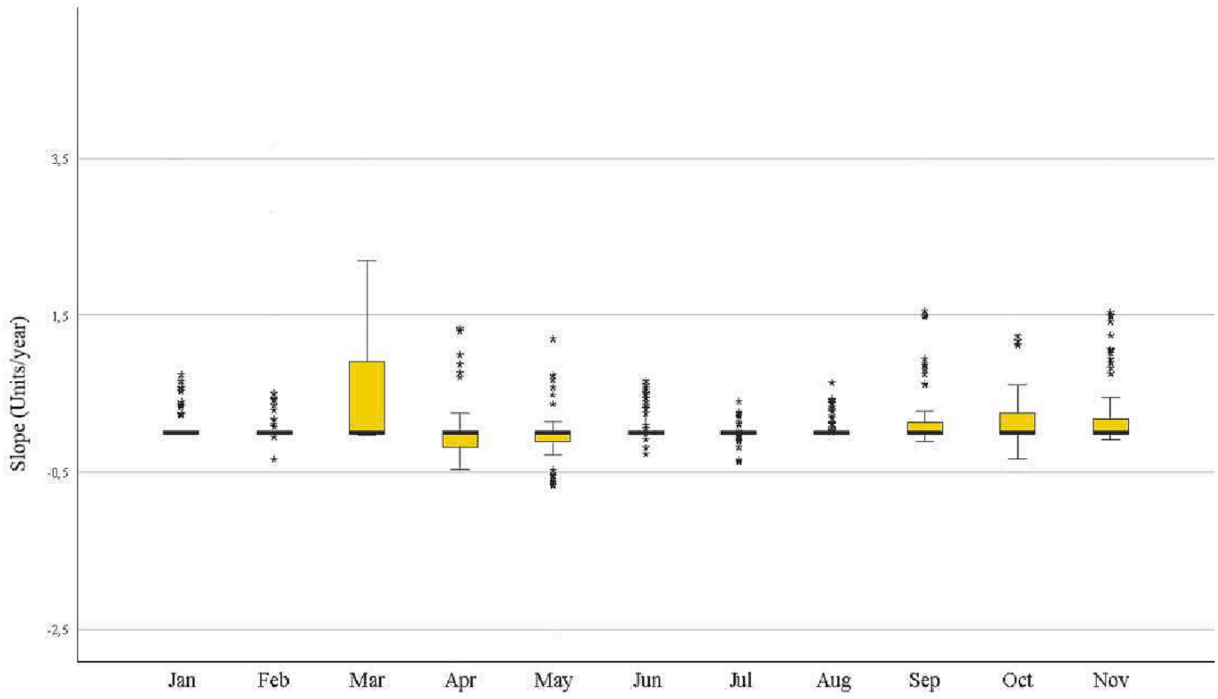

Fig. 4. Boxplot for monthly trend values in the State of California. The black line in the boxes (interquartile range) shows the slope of the median value for the whole State.

in northern California. This is directly related to recent research showing a slightly negative trend in mean temperature (Cordero et al., 2011; González-Pérez et al., 2022a) and a positive trend in rainfall over the northern half of the State of California (González-Pérez et al., 2022b). The highest negative values (-1.2 units year^{-1}) are observed in the vicinity of the Sacramento Valley, Los Banos and San Francisco. This is consistent with previous studies and projections for the second half of the 21st century, where "critically dry" water is 8% more frequent in the Sacramento Valley and 32% more often in the San Joaquin Valley (Dettinger and Cayan, 2014; MacDonald et al., 2008). In May, the northern areas with negative trends (Fig. 7) decrease, but the negative values of the Ombroxeric Index increase. In particular, negative values (−1.2 units year^{-1}) are observed at Yreka along with the Klamath Mountains (−1.6 units year^{-1}). A negative trend (−0.4 units year^{-1}) is also observed in the south and around Mount Whitney.

June, the first month of summer, is the one with the highest trend values. The values found in the southern Sierra Nevada (−1 units year^{-1}) are significant and increase as we approach the areas around Bridgeport (+4 units year^{-1}) and Lake Tahoe (+2.5 units year^{-1}). This positive trend in the Ombroxeric Index in this area is maintained in July and August, and only extends to the northern part of the State in June (Fig. 7). Negative trends are only observed in the Sacramento Valley and the surrounding areas of Santa Rosa, Cloverdale and Redding (−1 units year^{-1}). Comparable results are found for the summer period. Positive

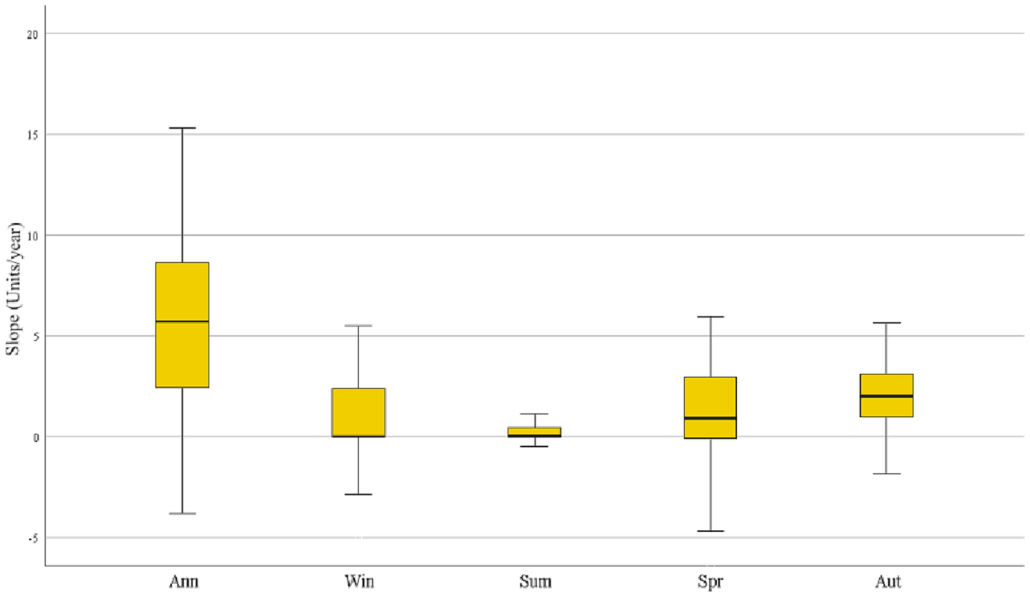

Fig. 5. Boxplot for seasonal and annual trend values in the State of California. The black line in the boxes (interquartile range) shows the slope of the median value for the whole State.

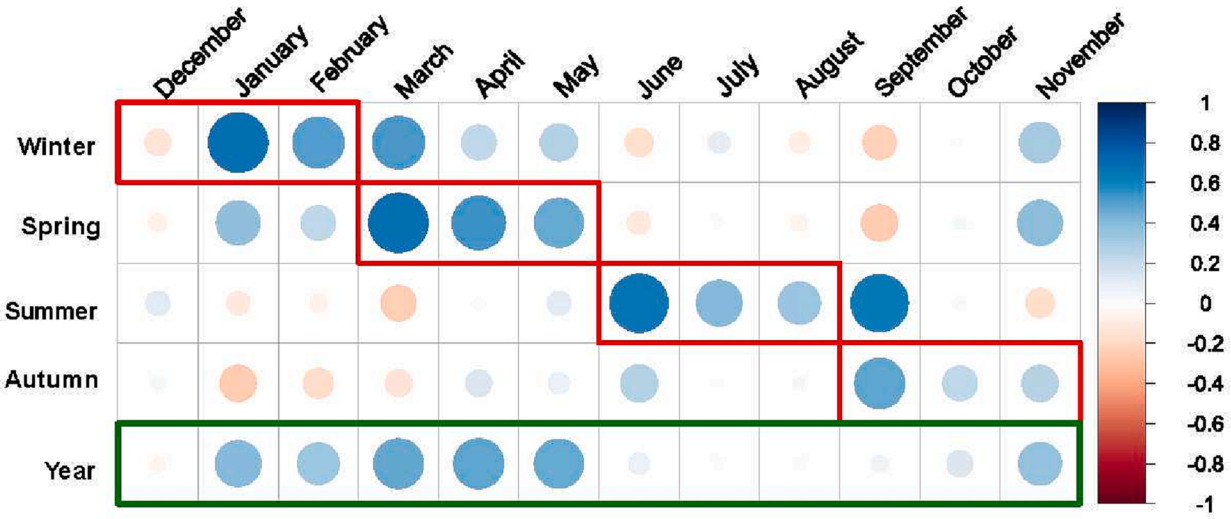

Fig. 6. Pearson correlation values crossing the Sen slopes on a monthly, seasonal and annual basis. The wider the circle, the higher the absolute correlation value. The red lines marked the months that structure the season, while the green lines represent the year. (For interpretation of the references to colour in this figure legend, the reader is referred to the web version of this article.)

trends were found in the same areas as in June. However, during this season the trend values are higher, with Bridgeport and adjacent areas reaching values of +5 units year^{-1} and Lake Tahoe reaching values of +4 units year^{-1}. It should be noted that during this season, positive trends of up to +4 units year^{-1} occurred in San Jacinto and the Laguna Mountains.

Moving to our results in September, we can see that the summer trend continues in the north of the State. The largest significant positive trends are seen in areas such as Susanville, Downieville, with +2 units year^{-1} and the Cascade ranges with +1.75 units year^{-1}. This positive trend extends to the southern Sierra Nevada (+0.5 units year^{-1}). In October comparable results are found to those in previous months. Positive trends in the Ombroxeric Index are found in most of the territories. Particularly, the highest values are found in San Jose, Santa Cruz and San Francisco (+0.8 units year^{-1}). On the other hand, negative trends are revealed in the southern coastal areas around Los Angeles and Long Beach (-0.4 units year^{-1}). Instead, the November results did not show any trends in northern California (Fig. 7). Instead, positive trends were observed in the southern parts of the State. Riverside, Long Beach and Los Angeles are the territories that showed the highest values in this month (+3.6 units year^{-1}). Positive trends, but of a lesser extent, are found in the southern Sierra Nevada (+1.5 units year^{-1}) and the Mojave Desert (+1.2 units year^{-1}).

3.2.2. Seasonal trends

Fig. 6 shows the correlation of each month with the seasons and at the annual level. In the case of spring, March is the month most correlated with the trend increases observed in that season. Particularly large increases in the Ombroxeric Index are observed in the Mojave Desert and in the city of Los Angeles (+4.5 units year^{-1}) and its surroundings (Fig. 7). Positive trends are also observed in the Rafael Mountains (+3.6 units year^{-1}) and the southern Sierra Nevada (+1.8 units year^{-1}). However, negative trends are found in Eureka (−1.8 units year^{-1}), Crescent City and the Klamath Mountains in the northwest, and an

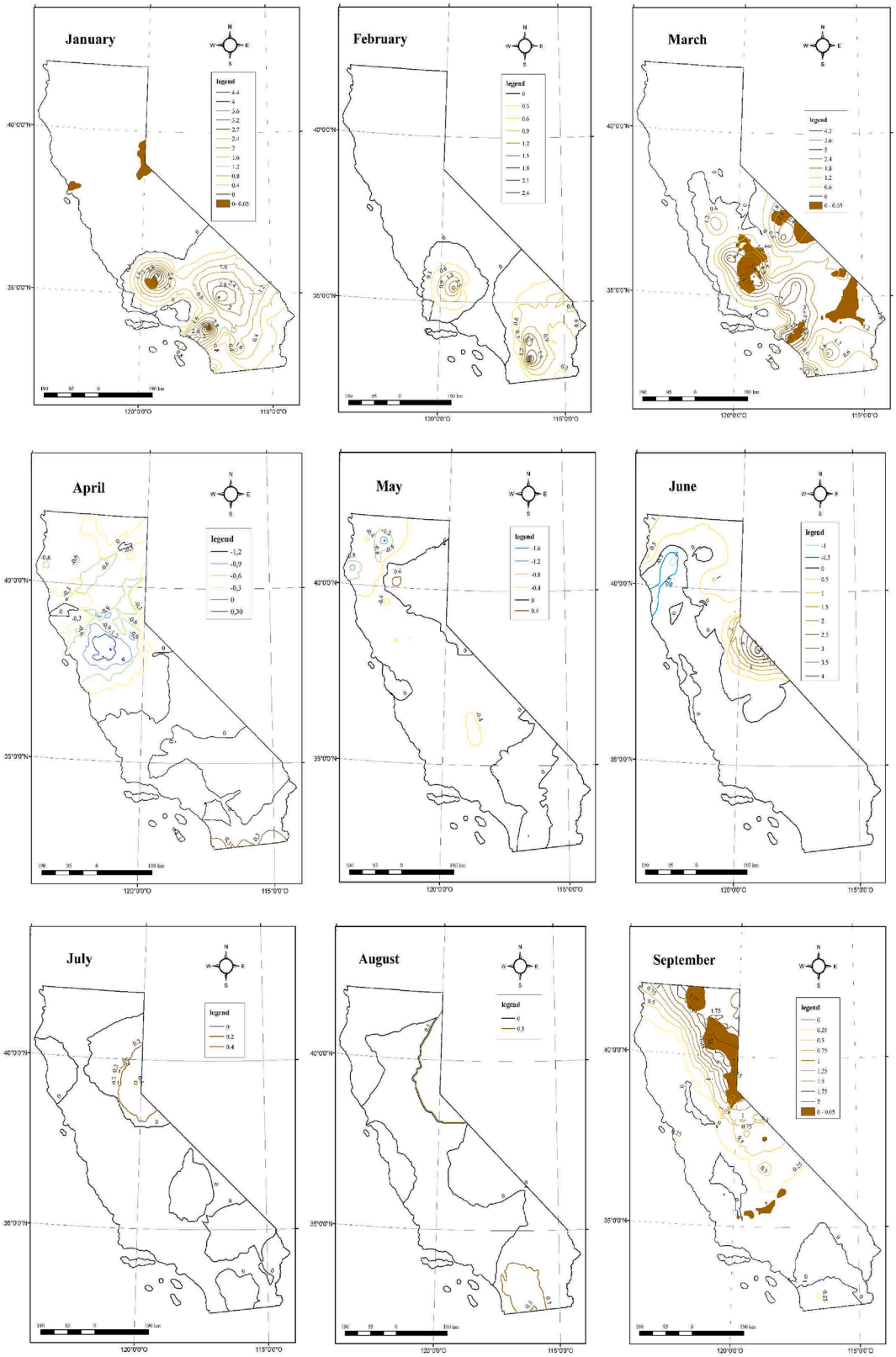

Fig. 7. Trends in the Ombroxeric Index (units year^{-1}) on a monthly, seasonal and annual basis. Brown areas indicate positive statistical significance at the 95% confidence level.

inflow to San Francisco Bay (-0.9 units year^{-1}) extending to Sacramento and surrounding areas. This is fairly consistent with other research that have found drier-than-normal conditions in May, June, and July (Rippey, 2015).

Comparable results are found for the summer period. We found positive trends in the same territories as in June. Furthermore, this

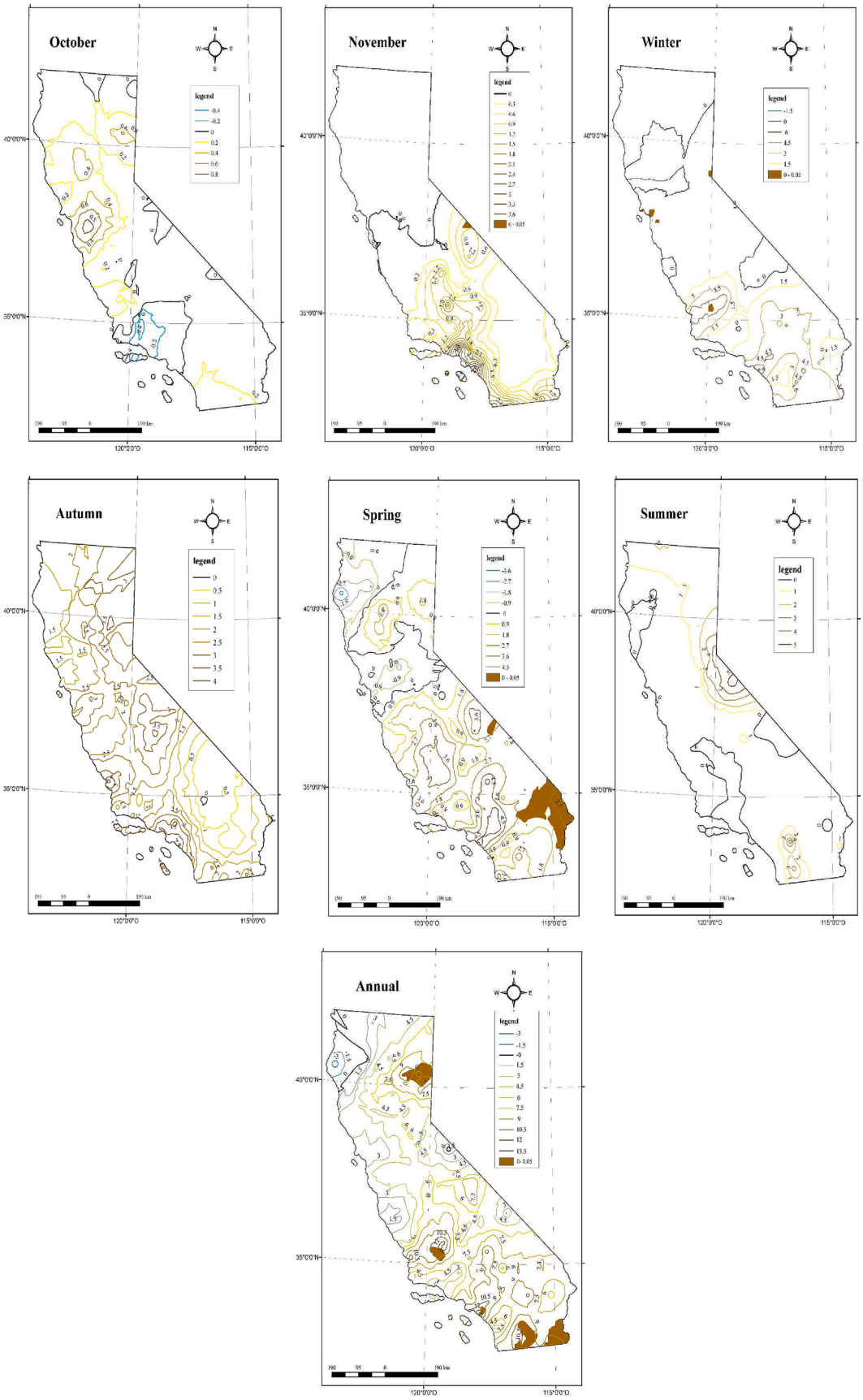

Fig. 7. (*continued*).

month shows the highest values of positive correlation in this season (Fig. 6). However, in this season the trend values are higher, with Bridgeport and adjacent areas reaching values of +5 units year^{-1} and Lake Tahoe reaching values of +4 units year^{-1}. It should be noted that during this season, positive trends of up to +4 units year^{-1} occurred in San Jacinto and the Laguna Mountains. These positive trends could lead to significant vegetation losses due to fires, as it has been seen that the decrease in relative humidity (RH), during times of high temperatures favours its spread, e.g. in the Klamath Mountains (Estes et al., 2017).

In autumn clear increases are found throughout the State (Fig. 7). The highest increases in this season are obtained in the Sierra Nevada territories from the north to the south of the State. In this case bioclimatic drought thrives in mountainous areas of California such as Susanville (+3.5 units year^{-1}), Downieville (+2.5 units year^{-1}), Independence (+3 units year^{-1}), Mount Whitney (+3.5 units year^{-1}), and the San Rafael Ranges (+1.5 units year^{-1}). This is supported by other research that showed a correlation between the Palmer Drought Severity Index (PDSI) and peak soil moisture in late summer and autumn across much of the western United States (Littell et al., 2016). It is important to mention that this season is critical for wildfires, because it is the beginning of the transition to the wet season, and for future projections (McEvoy et al., 2020).

Previous studies have found that a more water-limited regime is projected due to substantial decrease in precipitation in spring and autumn (González-Pérez et al., 2022b; McEvoy et al., 2020) with increased evapotranspiration that will further increase the imbalance between these two (McEvoy et al., 2020).

Analysing winter trends, we observe an increase in bioclimatic drought in the south of the State, as well as at the monthly level. It is worth noting that during this season values of (+6 units year^{-1}) are reached in the areas surrounding San Diego and Los Angeles. California's drought relationship with ENSO (El Niño-Southern Oscillation) has led to a change in the State's drought risk in the 21st century, mainly due to winter moisture (Allen and Anderson, 2018). Indeed, persistent negative Pacific Decadal Oscillation (PDO) conditions (Newman et al., 2016), consistent with the amplification evidence can be linked to excessively wet winters in California. In fact, González-Pérez et al. (2022b) showed that the PDO and precipitation in December are highly correlated. Furthermore, the western U.S is likely to experience intensified and extreme hydrological cycles (Simon Wang et al., 2017).

3.2.3. Annual trends

Finally, according to the annual results, positive trends in the Ombroxeric Index were detected in most of the State (Fig. 7). In addition, the period from January to May showed the highest positive correlation value with the positive annual trend of the ombroxeric drought (Fig. 6). The main increases are found in the southern areas of the State. In these zones, wind has a significant impact on California's drought conditions. Strong winds can cause rapid evaporation of soil moisture, leading to drought conditions. Additionally, strong winds can exacerbate wildfires, which are a significant contributor to drought settings (Littell et al., 2016). California's Santa Ana winds are known to be particularly dangerous and are linked to teleconnection patterns (Cardil et al., 2021). They are also hot and dry and can quickly spread wildfires, causing significant environmental damage and increasing drought (Guzman-Morales and Gershunov, 2019; Raphael, 2003). Furthermore, recent research has shown that drought periods are characterised by higher temperatures and lower relative humidity (RH) and wind speed, compared to non-drought periods (Lee et al., 2023).

Increases are found over the Sierra Nevada territories such as Bakersfield (+13 units year^{-1}), Owens Lake and Mount Whitney (+7 units year^{-1}), Nevada City and Lake Tahoe (+9 units year^{-1}), and remarkably the trend in these areas is statistically significant (Fig. 7). This is consistent with previous research showing decreases in the value of drought indices such as the Palmer Drought Severity Index (PSDI), the Palmer Hydrological Drought Index (PHDI) and the Palmer Moisture Anomaly Index (Z-Index). Five-year results from U.S. drought monitoring show comparable results to our trend analysis (U.S. Environmental Protection Agency, 2022). In fact, this supports our results suggesting an increase (+6 units year^{-1}) in the frequency of drought occurrence (Fig. 5), except for the two wettest regions (North Coast Drainage and Sacramento Drainage) (He and Gautam, 2016). Indeed, our results showed negative trends in the northern coastal areas of Eureka (−3 units year^{-1}) and the Coast Ranges (−1.5 units year^{-1}).

Due to the diversity of California's vegetation, the response to drought may differ. This is the case in a study where a high correlation between PDSI and NDVI was observed in the southern parts, implying a high sensitivity of chaparral, desert scrub, and grasslands to increasingly dry and warm conditions in this already arid environment (Dong et al., 2019a), where, according to our results, bioclimatic drought will become more frequent and severe. As we have observed, there will be a recurrent tendency towards drought in spring and almost all months, especially in this southern part of the State.

In brief, the trend analysis showed regional differences in the trends of the Ombroxeric Index while some areas show positive trends, indicating worsening drought conditions, others show no significant trend. This suggests that the severity of bioclimatic drought varies across different regions of California. The annual trend analysis indicates that the majority of meteorological stations (82%) exhibit positive trends in the Ombroxeric Index. This suggests a general increase in bioclimatic drought severity over the study period. These positive trends observed in the Ombroxeric Index indicate a potential long-term increase in drought conditions in California. This could have implications for water resource management, agricultural practices, and drought preparedness measures in the State. Moreover, the increasing frequency and severity of drought conditions could have a significant impact on chaparral, desert scrub, grasslands, and other vegetation types, such as coniferous species (González-Pérez et al., 2023) leading to changes in their distribution and habitat suitability.

4. Conclusions

In this paper, monthly, seasonal and annual bioclimatic drought has been investigated for the first time applying the Ombroxeric Index for the entire State of California (1980–2016). Its validity and applicability at different scales have been tested, with results consistent with previous research. Trend analysis was also carried out using both modified Mann-Kendall and Sen's slopes. The trends were presented in maps resulting from the Empirical Bayesian Interpolation technique. From these results we can conclude the following:

-Annually, California shows a wide range of ombroxeric levels, varying from upper strong dry in the northern part of the State to lower weak arid in both the Sonora and Mojave deserts. Trend results show increases throughout the State, being particularly high (+13 units year^{-1}) around Bakersfield although decreases appear (−3 units year^{-1}) in the surrounding area of Eureka.

- Focusing on monthly values, June, July and August are the months that show the highest levels of the Ombroxeric Index (lower ultra-hyperarid), particularly in southern California. Indeed June, shows positive trends (+4 units year^{-1}) in Lake Tahoe and in the northern territories of the State and it is most related to the summer positive trends. However, the trends for the months of July and August do not represent major variations for the study period, as there is no trend in most of the area.

-January, March and November are the months with the highest values of positive trends of up to +4.4 units year^{-1}, particularly in the southern part of the State (Sonora and Mojave deserts). Meanwhile, September have shown remarkably positive trends in the north-eastern areas. In addition, these are the months most closely correlated with the trend of the respective seasons to which they belong.

- Seasonally, California shows a gradual increase in bioclimatic drought. Thus, in the winter months, ombroxericity is isolated to the

southernmost part of the State, whose highest level is upper strong semiarid. In spring there is a gradual increase in bioclimatic drought. which does not reached in the highest areas of the Sierra Nevada and the north-western coast of the State. The maximum level reached in this season is upper ultrahyperarid. In summer, the highest OXI values are attained throughout the territory studied, with the lower ultrahyperarid level dominating in the southern zone and in both central valleys. In autumn, bioclimatic drought is observed throughout the State. In addition, the extent of hyperarid and ultrahyperarid ombroxerotypes dominates in the southern half of California. Seasonal trends provide positive values for the Ombroxeric Index over most of California, although there are negative trends in spring in areas of the west coast such as the Eureka and the Klamath Mountains.

Although it is true that on a monthly and seasonal scale, there are negative trends for this index, during the period studied there is a clear increase in bioclimatic drought, which may lead to variations in the loss of natural vegetation in California, and is directly related to the increase and severity of fires, as has been mentioned in other studies.

Knowing the levels and classifying the territories of California with the values of bioclimatic drought that we have shown, will make it possible to carry out a study of the types of vegetation that can develop in each of these levels in the face of future climate change scenarios. For this reason, it is important to know the evolution of the index in the context of climate change, in order to identify the vegetation that could survive in the new conditions. It is therefore necessary to stress the importance of studying the future relationship between bioclimatic drought and vegetation, and what is more, other aspects such as land use, human activity, etc.

CRediT authorship contribution statement

A. González-Pérez: Data curation, Formal analysis, Funding acquisition, Investigation, Methodology, Software, Visualization, Writing – original draft, Writing – review & editing. **R. Álvarez-Esteban:** Data curation, Formal analysis, Resources, Software, Validation, Visualization, Writing – review & editing. **Alejandro Velázquez:** Investigation, Writing – original draft, Writing – review & editing. **A. Penas:** Conceptualization, Resources, Supervision, Validation, Visualization, Writing – review & editing. **S. del Río:** Conceptualization, Project administration, Resources, Supervision, Validation, Visualization, Writing – review & editing.

Declaration of Competing Interest

The authors declare the following financial interests/personal relationships which may be considered as potential competing interests:

Alejandro González Pérez reports financial support was provided by Junta de Castilla y León Consejería de Educación.

The remaining authors declare that they have no known competing financial interests or personal relationships that could have appeared to influence the work reported in this paper.

Data availability

Data will be made available on request.

Acknowledgements

This paper was supported by the *European Regional Development Fund* (ERDF) and the Junta de Castilla y León (JCyL). The grant was awarded to the first author and included in a Fellowship Scheme for a Doctoral Training Program: *Orden de 12 de diciembre de 2019 de la Consejería de Educación (extracto publicado en el B.O.C. y L. n.° 245, de 23 de diciembre. BDNS (Identifi.): 487971*. University of Leon. Authors would like to thank Ruth J.R. Winter for her advice on English terminology.

References.

Aghelpour, P., Varshavian, V., 2021. Forecasting different types of droughts simultaneously using multivariate standardized precipitation index (MSPI), MLP neural network, and imperialistic competitive algorithm (ICA). Complexity 2021, 1–16. https://doi.org/10.1155/2021/6610228.

Ajjur, S.B., Al-Ghamdi, S.G., 2021. Evapotranspiration and water availability response to climate change in the Middle East and North Africa. Clim. Change 166, 1–18. https://doi.org/10.1007/S10584-021-03122-Z/FIGURES/7.

Allen, R.J., Anderson, R.G., 2018. 21st century California drought risk linked to model fidelity of the El Niño teleconnection. NPJ Clim. Atmos. Sci. 1 (1), 1–14. https://doi.org/10.1038/s41612-018-0032-x.

Álvarez Santacoloma, A., Álvarez-santacoloma, A., Breogán FERREIRO-LERA, G., González-pérez, A., Penas Merino, Á., Del Río González, S., 2022. Bioclimatic characterization of Northwest Spain (Asturias, Galicia and León). Int. J. Geobot. Res. 63–80 https://doi.org/10.5616/ijgr.

Anderson, M.C., Zolin, C.A., Sentelhas, P.C., Hain, C.R., Semmens, K., Tugrul Yilmaz, M., Gao, F., Otkin, J.A., Tetrault, R., 2016. The Evaporative Stress Index as an indicator of agricultural drought in Brazil: an assessment based on crop yield impacts. Remote Sens. Environ. 174, 82–99. https://doi.org/10.1016/J.RSE.2015.11.034.

Bachmair, S., Kohn, I., Stahl, K., 2015. Exploring the link between drought indicators and impacts. Nat. Hazards Earth Syst. Sci. 15 (6), 1381–1397. https://doi.org/10.5194/nhess-15-1381-2015.

Bachmair, S., Stahl, K., Collins, K., Hannaford, J., Acreman, M., Svoboda, M., Knutson, C., Smith, K.H., Wall, N., Fuchs, B., Crossman, N.D., Overton, I.C., 2016. Drought indicators revisited: the need for a wider consideration of environment and society. WIREs Water 3 (4), 516–536. https://doi.org/10.1002/wat2.1154.

Baguskas, S.A., Still, C.J., Fischer, D.T., D'Antonio, C.M., King, J.Y., 2016. Coastal fog during summer drought improves the water status of sapling trees more than adult trees in a California pine forest. Oecologia 181, 137–148. https://doi.org/10.1007/S00442-016-3556-Y/FIGURES/4.

Barbour, M.G., Keeler-Wolf, T., Schoenherr, A.A., 2007. Terrestrial vegetation of California, Terrestrial Vegetation of California. https://doi.org/10.2307/3897373.

Blöschl, G., Hall, J., Viglione, A., Perdigão, R.A.P., Parajka, J., Merz, B., Lun, D., Arheimer, B., Aronica, G.T., Bilibashi, A., Boháč, M., Bonacci, O., Borga, M., Čanjevac, I., Castellarin, A., Chirico, G.B., Claps, P., Frolova, N., Ganora, D., Gorbachova, L., Gül, A., Hannaford, J., Harrigan, S., Kireeva, M., Kiss, A., Kjeldsen, T.R., Kohnová, S., Koskela, J.J., Ledvinka, O., Macdonald, N., Mavrova-Guirguinova, M., Mediero, L., Merz, R., Molnar, P., Montanari, A., Murphy, C., Osuch, M., Ovcharuk, V., Radevski, I., Salinas, J.L., Sauquet, E., Šraj, M., Szolgay, J., Volpi, E., Wilson, D., Zaimi, K., Živković, N., 2019. Changing climate both increases and decreases European river floods. Nature 573 (7772), 108–111. https://doi.org/10.1038/s41586-019-1495-6.

Brown, J.F., Wardlow, B.D., Tadesse, T., Hayes, M.J., Reed, B.C., 2013. The Vegetation Drought Response Index (VegDRI): A New Integrated Approach for Monitoring Drought Stress in Vegetation. https://doi.org/10.2747/1548-1603.45.1.16 45, 16–46. https://doi.org/10.2747/1548-1603.45.1.16.

Cardil, A., Rodrigues, M., Ramirez, J., de-Miguel, S., Silva, C.A., Mariani, M., Ascoli, D., 2021. Coupled effects of climate teleconnections on drought, Santa Ana winds and wildfires in southern California. Sci. Total Environ. 765, 142788 https://doi.org/10.1016/j.scitotenv.2020.142788.

Center, W.R.C., 2000. Western regional climate center. Tuweep, Arizona Station Report, Reno, Nevada, USA.

Chang, H., Bonnette, M.R., 2016. Climate change and water-related ecosystem services: impacts of drought in California, USA. Ecosyst. Health Sustain. 2 https://doi.org/10.1002/EHS2.1254/SUPPL_FILE/TEHS_A_11879061_SM0003.DOCX.

Corbin, J.D., Thomsen, M.A., Dawson, T.E., D'Antonio, C.M., 2005. Summer water use by California coastal prairie grasses: fog, drought, and community composition. Oecologia 145 (4), 511–521. https://doi.org/10.1007/s00442-005-0152-y.

Cordero, E.C., Kessomkiat, W., Abatzoglou, J., Mauget, S.A., 2011. The identification of distinct patterns in California temperature trends. Clim. Change 108, 357–382. https://doi.org/10.1007/s10584-011-0023-y.

del Río, S., Penas, Á., Pérez González, A., Rivas-Martínez, S., 2018. Two new bioclimatic indexes to calculate aridity and dryness. An example for continental Spain. Botanique 4 (1), 25–27.

Dettinger, M., Cayan, D.R., 2014. Drought and the California delta - A matter of extremes. San Francisco Estuary and Watershed Science 12, 1–6. https://doi.org/10.15447/SFEWS.2014V12ISS2ART4.

Diffenbaugh, N.S., Swain, D.L., Touma, D., 2015. Anthropogenic warming has increased drought risk in California. Proc. Natl. Acad. Sci. 112 (13), 3931–3936. https://doi.org/10.1073/pnas.1422385112.

Diodato, N., De Guenni, L.B., Garcia, M., Bellocchi, G., 2019. Decadal oscillation in the predictability of Palmer Drought Severity Index in California. Climate 7 (1), 6.

Dong, L., Leung, L.R., 2021. Winter precipitation changes in California under global warming: contributions of CO_2, uniform SST warming, and SST change patterns. Geophys. Res. Lett. 48 https://doi.org/10.1029/2020GL091736 e2020GL091736.

Dong, C., MacDonald, G.M., Willis, K., Gillespie, T.W., Okin, G.S., Williams, A.P., 2019a. Vegetation responses to 2012–2016 drought in Northern and Southern California. Geophys. Res. Lett. 46 (7), 3810–3821. https://doi.org/10.1029/2019GL082137.

Dong, C., MacDonald, G., Okin, G.S., Gillespie, T.W., 2019b. Quantifying drought sensitivity of mediterranean climate vegetation to recent warming: a case study in Southern California. Remote Sens. (Basel) 11 (24), 2902. https://doi.org/10.3390/rs11242902.

Dracup, J.A., Lee, K.S., Paulson, E.G., 1980. On the definition of droughts. Water Resour. Res. 16 (2), 297–302. https://doi.org/10.1029/WR016i002p00297.

Environmental Systems Research Institute (ESRI), 2019. ARCGIS.

Estes, B.L., Knapp, E.E., Skinner, C.N., Miller, J.D., Preisler, H.K., 2017. Factors influencing fire severity under moderate burning conditions in the Klamath Mountains, northern California, USA. Ecosphere 8. https://doi.org/10.1002/ecs2.1794.

Famiglietti, J.S., Lo, M., Ho, S.L., Bethune, J., Anderson, K.J., Syed, T.H., Swenson, S.C., De Linage, C.R., Rodell, M., 2011. Satellites measure recent rates of groundwater depletion in California's Central Valley. Geophys. Res. Lett. 38 https://doi.org/10.1029/2010GL046442.

Ferreiro-Lera, G.B., Penas, A., del Río, S., 2022. Bioclimatic drought trend study through the application of the ombroxeric index. A case study: the province of León (Spain). J. Maps. https://doi.org/10.1080/17445647.2022.2101949/SUPPL_FILE/TJOM_A_2101949_SM2078.ZIP.

Flint, L.E., Flint, A.L., Mendoza, J., Kalansky, J., Ralph, F.M., 2018. Characterizing drought in California: new drought indices and scenario-testing in support of resource management. Ecol. Process. 7 https://doi.org/10.1186/s13717-017-0112-6.

Friedman, D.G., 1957. The prediction of long-continuing drought in south and souhtwest Texas. Occational Papers in Meteorology No 1, 182.

Gamelin, B.L., Feinstein, J., Wang, J., Bessac, J., Yan, E., Kotamarthi, V.R., 2022. Projected U.S. drought extremes through the twenty-first century with vapor pressure deficit. Sci. Rep. 12 (1), 1–15. https://doi.org/10.1038/s41598-022-12516-7.

Ghazal, N.K., 2019. Comparison of three interpolation methods for the average monthly temperature in the south of Iraqi zone. Iraqi. J. Phys. 11 https://doi.org/10.30723/ijp.v11i21.368.

Gocic, M., Trajkovic, S., 2013. Analysis of changes in meteorological variables using Mann-Kendall and Sen's slope estimator statistical tests in Serbia. Glob. Planet Change 100, 172–182. https://doi.org/10.1016/j.gloplacha.2012.10.014.

González-Pérez, A., Álvarez-Esteban, R., Penas, Á., del Río, S., 2022a. Analysis of recent mean temperature trends and relationships with teleconnection patterns in California (U.S.). Appl. Sci. 12, 5831. https://doi.org/10.3390/app12125831.

González-Pérez, A., Álvarez-Esteban, R., Penas, A., del Río, S., 2022b. Analysis of recent rainfall trends and links to teleconnection patterns in California (U.S.). J. Hydrol. (Amst) 612, 128211. https://doi.org/10.1016/J.JHYDROL.2022.128211.

González-Pérez, A., Álvarez-Esteban, R., Penas, Á., del Río, S., 2023. Bioclimatic characterisation of specific native Californian Pinales and their future suitability under climate Change. Plants 12, 1966. https://doi.org/10.3390/plants12101966.

Goss, M., Swain, D.L., Abatzoglou, J.T., Sarhadi, A., Kolden, C.A., Williams, A.P., Diffenbaugh, N.S., 2020. Climate change is increasing the likelihood of extreme autumn wildfire conditions across California. Environ. Res. Lett. 15, 94016. https://doi.org/10.1088/1748-9326/AB83A7.

Gribov, A., Krivoruchko, K., 2020. Empirical Bayesian kriging implementation and usage. Sci. Total Environ. 722, 137290 https://doi.org/10.1016/j.scitotenv.2020.137290.

Griffin, D., Anchukaitis, K.J., 2014. How unusual is the 2012–2014 California drought? Geophys. Res. Lett. 41 (24), 9017–9023. https://doi.org/10.1002/2014GL062433.

Gupta, A., Kamble, T., Machiwal, D., 2017. Comparison of ordinary and Bayesian kriging techniques in depicting rainfall variability in arid and semi-arid regions of north-west India. Environ. Earth Sci. 76, 1–16. https://doi.org/10.1007/S12665-017-6814-3/FIGURES/5.

Guzman-Morales, J., Gershunov, A., 2019. Climate change suppresses Santa Ana winds of southern California and sharpens their seasonality. Geophys. Res. Lett. 46 (5), 2772–2780. https://doi.org/10.1029/2018GL080261.

Hamlet, A.F., Mote, P.W., Clark, M.P., Lettenmaier, D.P., 2005. Effects of temperature and precipitation variability on snowpack trends in the Western United States. J. Clim. 18, 4545–4561. https://doi.org/10.1175/JCLI3538.1.

Haque Mondol, M.A., Zhu, X., Dunkerley, D., Henley, B.J., 2022. Technological drought: a new category of water scarcity. J. Environ. Manage. 321, 115917 https://doi.org/10.1016/J.JENVMAN.2022.115917.

Harou, J.J., Medellín-Azuara, J., Zhu, T., Tanaka, S.K., Lund, J.R., Stine, S., Olivares, M. A., Jenkins, M.W., 2010. Economic consequences of optimized water management for a prolonged, severe drought in California. Water Resour. Res. 46 https://doi.org/10.1029/2008WR007681.

He, M., Gautam, M., 2016. Variability and trends in precipitation, temperature and drought indices in the state of California. Hydrology. 3 (2), 14. https://doi.org/10.3390/hydrology3020014.

Heim, R.R., 2002. A review of twentieth-century drought indices used in the United States. Bull. Am. Meteorol. Soc. 83 (8), 1149–1166. https://doi.org/10.1175/1520-0477-83.8.1149.

Herrera-Estrada, J.E., Satoh, Y., Sheffield, J., 2017. Spatiotemporal dynamics of global drought. Geophys. Res. Lett. 44 (5), 2254–2263. https://doi.org/10.1002/2016GL071768.

Huang, S., Leng, G., Huang, Q., Xie, Y., Liu, S., Meng, E., Li, P., 2017. The asymmetric impact of global warming on US drought types and distributions in a large ensemble of 97 hydro-climatic simulations. Sci. Rep. 7 https://doi.org/10.1038/s41598-017-06302-z.

Kam, J., Sheffield, J., 2016. Increased drought and pluvial risk over california due to changing oceanic conditions. J. Clim. 29, 8269–8279. https://doi.org/10.1175/JCLI-D-15-0879.1.

Karmeshu, N., 2015. Trend Detection in Annual Temperature & Precipitation using the Mann Kendall Test – A Case Study to Assess Climate Change on Select States in the Northeastern United States. University of Pennsylvania.

Keen, R.M., Voelker, S.L., Wang, S.-Y., Bentz, B.J., Goulden, M.L., Dangerfield, C.R., Reed, C.C., Hood, S.M., Csank, A.Z., Dawson, T.E., Merschel, A.G., Still, C.J., 2022. Changes in tree drought sensitivity provided early warning signals to the California drought and forest mortality event. Glob. Chang. Biol. 28 (3), 1119–1132. https://doi.org/10.1111/gcb.15973.

Krivoruchko, K., Gribov, A., 2019. Evaluation of empirical Bayesian kriging. Spat Stat. 32, 100368 https://doi.org/10.1016/j.spasta.2019.100368.

Krivoruchko, K., 2012. Empirical Bayesian Kriging. ESRI Press Fall 2012, 6–10.

Kukal, M., Irmak, S., 2016. Long-term patterns of air temperatures, daily temperature range, precipitation, grass-reference evapotranspiration and aridity index in the USA Great Plains: part I. Spatial trends. J. Hydrol. (Amst). 542, 953–977. https://doi.org/10.1016/j.jhydrol.2016.06.006.

Lee, H.J., Bell, M.L., Koutrakis, P., 2023. Drought and ozone air quality in California: identifying susceptible regions in the preparedness of future drought. Environ. Res. 216, 114461 https://doi.org/10.1016/j.envres.2022.114461.

Li, Y., Hernandez, J.H., Aviles, M., Knappett, P.S.K., Giardino, J.R., Miranda, R., Puy, M. J., Padilla, F., Morales, J., 2020. Empirical Bayesian Kriging method to evaluate inter-annual water-table evolution in the Cuenca Alta del Río Laja aquifer, Guanajuato, México. J. Hydrol. (Amst) 582, 124517. https://doi.org/10.1016/j.jhydrol.2019.124517.

Lisonbee, J., Ossowski, E., Muth, M., Deheza, V., Sheffield, A., 2022. Preparing for long-term drought and aridification. Bull. Am. Meteorol. Soc. 103, E821–E827. https://doi.org/10.1175/BAMS-D-21-0321.1.

Littell, J.S., Peterson, D.L., Riley, K.L., Liu, Y., Luce, C.H., 2016. A review of the relationships between drought and forest fire in the United States. Glob. Chang. Biol. 22, 2353–2369. https://doi.org/10.1111/GCB.13275.

Liu, Q., Shepherd, B., Li, C., 2020. Presiduals: an R package for residual analysis using probability-scale residuals. J. Stat. Softw. 94, 1–27. https://doi.org/10.18637/jss.v094.i12.

Luteyn, J.L., Hickman, J.C., 1993. The Jepson manual: higher plants of California. Brittonia 45 (4), 343. https://doi.org/10.2307/2807611.

MacDonald, G.M., Kremenetski, K.V., Hidalgo, H.G., 2008. Southern California and the perfect drought: simultaneous prolonged drought in southern California and the Sacramento and Colorado River systems. Quat. Int. 188, 11–23. https://doi.org/10.1016/J.QUAINT.2007.06.027.

Marcos-Garcia, P., Lopez-Nicolas, A., Pulido-Velazquez, M., 2017. Combined use of relative drought indices to analyze climate change impact on meteorological and hydrological droughts in a Mediterranean basin. J. Hydrol. (Amst) 554, 292–305. https://doi.org/10.1016/j.jhydrol.2017.09.028.

McEvoy, D.J., Pierce, D.W., Kalansky, J.F., Cayan, D.R., Abatzoglou, J.T., 2020. Projected changes in reference evapotranspiration in California and Nevada: implications for drought and wildland fire danger. Earths Fut. 8 https://doi.org/10.1029/2020EF001736 e2020EF001736.

Meseguer-Ruiz, O., Sarricolea, P., 2017. Detection of non-homogeneities in daily precipitation series in central and southern Chile. Interciencia 42, 242–249.

Mirabbasi, R., Anagnostou, E.N., Fakheri-Fard, A., Dinpashoh, Y., Eslamian, S., 2013. Analysis of meteorological drought in northwest Iran using the Joint Deficit Index. J. Hydrol. (Amst) 492, 35–48. https://doi.org/10.1016/J.JHYDROL.2013.04.019.

Mishra, A.K., Singh, V.P., 2010. A review of drought concepts. J. Hydrol. (Amst) 391 (1-2), 202–216. https://doi.org/10.1016/j.jhydrol.2010.07.012.

Mukherjee, S., Mishra, A., Trenberth, K.E., 2018. Climate change and drought: a perspective on drought indices. Curr. Clim. Change Rep. 4, 145–163. https://doi.org/10.1007/S40641-018-0098-X/FIGURES/3.

Newman, M., Alexander, M.A., Ault, T.R., Cobb, K.M., Deser, C., di Lorenzo, E., Mantua, N.J., Miller, A.J., Minobe, S., Nakamura, H., Schneider, N., Vimont, D.J., Phillips, A.S., Scott, J.D., Smith, C.A., 2016. The pacific decadal oscillation, revisited. J. Clim. 29, 4399–4427. https://doi.org/10.1175/JCLI-D-15-0508.1.

Otkin, J.A., Anderson, M.C., Hain, C., Svoboda, M., Johnson, D., Mueller, R., Tadesse, T., Wardlow, B., Brown, J., 2016. Assessing the evolution of soil moisture and vegetation conditions during the 2012 United States flash drought. Agric. For. Meteorol. 218–219, 230–242. https://doi.org/10.1016/J.AGRFORMET.2015.12.065.

Palmer, W.C., 1968. Keeping track of crop moisture conditions, nationwide: the new crop moisture index. Weatherwise 21 (4), 156–161. https://doi.org/10.1080/00431672.1968.9932814.

Patakamuri, S.K., O'Brien, N., 2021. Modified Versions of Mann Kendall and Spearman's Rho Trend Tests.

Pathak, T., Maskey, M., Dahlberg, J., Kearns, F., Bali, K., Zaccaria, D., 2018. Climate change trends and impacts on California agriculture: a detailed review. Agronomy 8 (3), 25. https://doi.org/10.3390/agronomy8030025.

Peña-Angulo, D., Gonzalez-Hidalgo, J.C., Sandonís, L., Beguería, S., Tomas-Burguera, M., López-Bustins, J.A., Lemus-Canovas, M., Martin-Vide, J., 2021. Seasonal temperature trends on the Spanish mainland: a secular study (1916–2015). Int. J. Climatol. 41 (5), 3071–3084. https://doi.org/10.1002/joc.7006.

Raphael, M.N., 2003. The Santa Ana Winds of California. Earth Interact 7. https://doi.org/10.1175/1087-3562(2003)007<0001:tsawoc>2.0.co;2.

Río, S.del, Iqbal, M.A., Cano-Ortiz, A., Herrero, L., Hassan, A., Penas, A., 2013. Recent mean temperature trends in Pakistan and links with teleconnection patterns. Int. J. Climatol. 33, 277–290. https://doi.org/10.1002/joc.3423.

Ríos Cornejo, D., Penas, Á., Álvarez-Esteban, R., del Río, S., 2015. Links between teleconnection patterns and mean temperature in Spain. https://doi.org/10.1007/s00704-014-1256-2.

Rippey, B.R., 2015. The U.S. drought of 2012. Weather Clim. Extrem. 10, 57–64. https://doi.org/10.1016/J.WACE.2015.10.004.

Rivas-Martínez, S., Rivas-Sáenz, S., Penas-Merino, A., 2011. Worldwide bioclimatic classification system. Global Geobotany 1, 1–638. https://doi.org/10.5616/gg110001.

Salimi, H., Asadi, E., Darbandi, S., 2021. Meteorological and hydrological drought monitoring using several drought indices. Appl. Water Sci. 11 https://doi.org/10.1007/s13201-020-01345-6.

Seager, R., Osborn, T.J., Kushnir, Y., Simpson, I.R., Nakamura, J., Liu, H., 2019. Climate variability and change of mediterranean-type climates. J. Clim. 32 (10), 2887–2915. https://doi.org/10.1175/JCLI-D-18-0472.1.

Sepulcre-Canto, G., Horion, S., Singleton, A., Carrao, H., Vogt, J., 2012. Development of a Combined Drought Indicator to detect agricultural drought in Europe. Nat. Hazards Earth Syst. Sci. 12 (11), 3519–3531. https://doi.org/10.5194/nhess-12-3519-2012.

Shukla, S., Safeeq, M., Aghakouchak, A., Guan, K., Funk, C., 2015. Temperature impacts on the water year 2014 drought in California. Geophys. Res. Lett. 42, 4384–4393. https://doi.org/10.1002/2015GL063666.

Simon Wang, S.Y., Yoon, J.H., Becker, E., Gillies, R., 2017. California from drought to deluge. Nat. Clim. Chang. 7, 465–468. https://doi.org/10.1038/NCLIMATE3330.

Song, X., Zhang, J., Zou, X., Zhang, C., AghaKouchak, A., Kong, F., 2019. Changes in precipitation extremes in the Beijing metropolitan area during 1960–2012. Atmos. Res. 222, 134–153. https://doi.org/10.1016/j.atmosres.2019.02.006.

Thom, H.C.S., 1966. Some methods of climatological analysis.

Thomas, B.F., Famiglietti, J.S., Landerer, F.W., Wiese, D.N., Molotch, N.P., Argus, D.F., 2017. GRACE groundwater drought index: evaluation of California Central Valley groundwater drought. Remote Sens. Environ. 198, 384–392. https://doi.org/10.1016/j.rse.2017.06.026.

Torregrosa, A., Taylor, M.D., Flint, L.E., Flint, A.L., 2013. Present, future, and novel Bioclimates of the San Francisco, California region. PLoS One 8, e58450. https://doi.org/10.1371/JOURNAL.PONE.0058450.

Trenberth, K.E., 2008. The impact of climate change and variability on heavy precipitation, floods, and droughts. Encycl. Hydrol. Sci. https://doi.org/10.1002/0470848944.hsa211.

U.S. Environmental Protection Agency, 2022. Climate Change Indicators: Drought [WWW Document].

Van Loon, A.F., Stahl, K., Di Baldassarre, G., Clark, J., Rangecroft, S., Wanders, N., Gleeson, T., Van Dijk, A.I.J.M., Tallaksen, L.M., Hannaford, J., Uijlenhoet, R., Teuling, A.J., Hannah, D.M., Sheffield, J., Svoboda, M., Verbeiren, B., Wagener, T., Van Lanen, H.A.J., 2016. Drought in a human-modified world: reframing drought definitions, understanding, and analysis approaches. Hydrol. Earth Syst. Sci. 20 (9), 3631–3650. https://doi.org/10.5194/hess-20-3631-2016.

Vicente-Serrano, S.M., Quiring, S.M., Peña-Gallardo, M., Yuan, S., Domínguez-Castro, F., 2020. A review of environmental droughts: increased risk under global warming? Earth Sci. Rev. 201, 102953 https://doi.org/10.1016/j.earscirev.2019.102953.

von Storch, H., 1995. Misuses of Statistical Analysis in Climate Research, in: Analysis of Climate Variability. https://doi.org/10.1007/978-3-662-03167-4_2.

Vu-Thanh, H., Ngo-Duc, T., Phan-Van, T., 2014. Evolution of meteorological drought characteristics in Vietnam during the 1961–2007 period. Theor. Appl. Climatol. 118, 367–375. https://doi.org/10.1007/S00704-013-1073-Z/FIGURES/6.

Warter, M.M., Singer, M.B., Cuthbert, M.O., Roberts, D., Caylor, K.K., Sabathier, R., Stella, J., 2021. Drought onset and propagation into soil moisture and grassland vegetation responses during the 2012–2019 major drought in Southern California. Hydrol. Earth Syst. Sci. 25, 3713–3729. https://doi.org/10.5194/HESS-25-3713-2021.

Weiskopf, S.R., Rubenstein, M.A., Crozier, L.G., Gaichas, S., Griffis, R., Halofsky, J.E., Hyde, K.J.W., Morelli, T.L., Morisette, J.T., Muñoz, R.C., Pershing, A.J., Peterson, D. L., Poudel, R., Staudinger, M.D., Sutton-Grier, A.E., Thompson, L., Vose, J., Weltzin, J.F., Whyte, K.P., 2020. Climate change effects on biodiversity, ecosystems, ecosystem services, and natural resource management in the United States. Sci. Total Environ. 733, 137782 https://doi.org/10.1016/J.SCITOTENV.2020.137782.

Williams, A.P., Seager, R., Abatzoglou, J.T., Cook, B.I., Smerdon, J.E., Cook, E.R., 2015. Contribution of anthropogenic warming to California drought during 2012–2014. Geophys. Res. Lett. 42 (16), 6819–6828. https://doi.org/10.1002/2015GL064924.

Xu, S., Yu, Z., Yang, C., Ji, X., Zhang, K., 2018. Trends in evapotranspiration and their responses to climate change and vegetation greening over the upper reaches of the Yellow River Basin. Agric. For. Meteorol. 263, 118–129. https://doi.org/10.1016/J.AGRFORMET.2018.08.010.

Yihdego, Y., Vaheddoost, B., Al-Weshah, R.A., 2019. Drought indices and indicators revisited. Arab. J. Geosci. 12 (3) https://doi.org/10.1007/s12517-019-4237-z.